

# User-Feedback-Driven Continual Adaptation for Vision-and-Language Navigation

Yongqiang Yu, Xuhui Li, Hazza Mahmood, Jinxing Zhou, Haodong Hong,  
Longtao Jiang, Zhiqiang Xu, Qi Wu, and Xiaojun Chang

**Abstract**—Vision-and-Language Navigation (VLN) requires agents to navigate complex environments by following natural-language instructions. General Scene Adaptation for VLN (GSA-VLN) shifts the focus from zero-shot generalization to continual, environment-specific adaptation, narrowing the gap between static benchmarks and real-world deployment. However, current GSA-VLN frameworks exclude user feedback, relying solely on unsupervised adaptation from repeated environmental exposure. In practice, user feedback offers natural and valuable supervision that can significantly enhance adaptation quality. We introduce a user-feedback-driven adaptation framework that extends GSA-VLN by systematically integrating human interactions into continual learning. Our approach converts user feedback—navigation instructions and corrective signals—into high-quality, environment-aligned training data, enabling efficient and realistic adaptation. A memory-bank warm-start mechanism further reuses previously acquired environmental knowledge, mitigating cold-start degradation and ensuring stable redeployment. Experiments on the GSA-R2R benchmark show that our method consistently surpasses strong baselines such as GR-DUET, improving navigation success and path efficiency. The memory-bank warm start stabilizes early navigation and reduces performance drops after updates. Results under both continual and hybrid adaptation settings confirm the robustness and generality of our framework, demonstrating sustained improvement across diverse deployment conditions.

**Index Terms**—Vision-Language Navigation, Embodied Artificial Intelligence, Continual Learning, User Feedback, Memory-based Adaptation, Human-Robot Interaction.

## I. INTRODUCTION

**V**ISION-AND-LANGUAGE Navigation (VLN) [1] has emerged as a core research problem in embodied intelligence. It requires autonomous agents to navigate complex indoor environments by following natural-language instructions [2], while jointly leveraging visual perception, language understanding [3], and spatial reasoning [1]. The ability to align linguistic guidance with visual observations and spatial context is widely regarded as fundamental to developing

Yongqiang Yu, Xuhui Li, Hazza Mahmood, Jinxing Zhou, Zhiqiang Xu, and Xiaojun Chang are with the Mohamed bin Zayed University of Artificial Intelligence (MBZUAI), Abu Dhabi, United Arab Emirates (e-mail: {yongqiang.yu, xuhui.li, hazza.mahmood, jinxing.zhou, zhiqiang.xu, xiaojun.chang}@mbzuai.ac.ae).

Haodong Hong is with the School of Electrical Engineering and Computer Science, The University of Queensland, Australia (e-mail: haodong.hong@uq.edu.au).

Longtao Jiang is with the University of Science and Technology of China (USTC), Hefei, China (e-mail: longtao.jiang@ustc.edu.cn).

Qi Wu is with the School of Computer Science, The University of Adelaide, Australia (e-mail: qi.wu01@adelaide.edu.au).

Xiaojun Chang is also with the University of Science and Technology of China (USTC), Hefei, China (e-mail: cxj@ustc.edu.cn).

Corresponding authors: Qi Wu (e-mail: qi.wu01@adelaide.edu.au) and Xiaojun Chang (e-mail: xiaojun.chang@mbzuai.ac.ae).

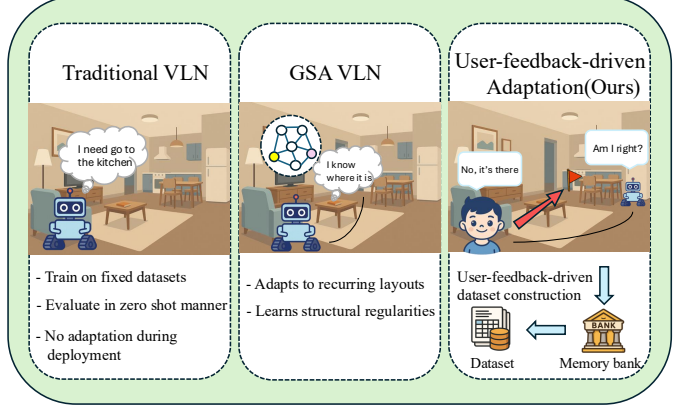


Fig. 1. Comparison between traditional VLN, GSA-VLN, and the proposed user-feedback-driven adaptation paradigm.

embodied systems [4] capable of assisting humans in everyday life. Examples include household robots that guide residents to frequently visited locations, elder-care assistants that help patients perform daily routines, and personal service robots that locate objects or reach designated destinations. In all these scenarios, agents must not only follow instructions once but also continually improve their navigation capability as they repeatedly operate within the same physical environment [5]–[7].

Despite remarkable progress [8] on benchmark datasets [1], [9]–[11], conventional VLN evaluation remains constrained by a fundamental limitation. Standard protocols typically adopt a zero-shot transfer setting [1], [2], in which agents are trained on a set of source environments and evaluated in novel, unseen targets [2], [12]–[14]. During evaluation, agents are explicitly prohibited from reusing experience gained through repeated exposure to the same scenes. While this setup provides a clean measure of generalization, it diverges substantially from real-world deployment conditions [11], [15], [16]. In practice, environments are often stable or evolve only gradually. For example, a household robot may navigate the same living room daily under slightly different instructions, or an office assistant may traverse the same floor plan over months of operation [17]. Ignoring accumulated navigation experience in such settings prevents agents from exploiting natural opportunities for continual improvement [5], [6]. As a result, current state-of-the-art models—trained once on static datasets—are unable to leverage the rich, repeated feedback that naturally arises during deployment [18].

To address this limitation, recent studies have explored Gen-

eral Scene Adaptation for Vision-and-Language Navigation (GSA-VLN) [19], which explicitly recognizes that long-term deployments offer new opportunities for continual learning. As shown in Fig. 1, traditional VLN focuses on one-shot instruction following in unseen scenes, whereas GSA-VLN enables agents to adapt to consistent environments through accumulated experience and memory-based updates. Within this paradigm, agents are encouraged to exploit stable spatial layouts, recurring visual observations, and regularized instruction patterns that naturally arise in persistent environments. A representative model in this direction is GR-DUET [19], which augments agents with environment-specific memory graphs that capture structural regularities. By leveraging such memory mechanisms, GR-DUET adapts more effectively than static models, illustrating the promise of GSA-VLN in bridging the gap between static training and dynamic, real-world operation.

Nevertheless, existing GSA-VLN approaches, including GR-DUET, remain constrained by a key assumption: adaptation arises solely from repeated environmental exposure, without incorporating explicit user feedback. Although GSA-VLN permits parameter updates through unsupervised learning, the supervision signal is limited to the agent’s own, often erroneous, navigation experiences. In realistic deployments, however, users naturally provide both navigation instructions and corrective feedback. Unlike unlabeled trajectories derived from failed attempts, such feedback is authentic, intent-aligned, and offers explicit supervision that cannot be easily replicated through unsupervised methods alone.

Building on GR-DUET, we extend the adaptation paradigm by incorporating user feedback as an additional source of supervision. Such feedback provides corrective guidance—indicating whether the agent has reached the intended goal or specifying the correct target location when it fails—thus complementing environment-driven learning. Unlike GR-DUET, which relies solely on repeated exposure, our approach reframes adaptation from being purely environment-driven to user-feedback-driven. This shift moves beyond the constraints of the GSA-VLN definition and establishes a new paradigm in which user interactions are systematically leveraged as a valuable source of supervision for continual improvement.

To realize this idea, we propose a user-feedback-driven adaptation framework for VLN, as illustrated in the right panel of Fig. 1. The framework consists of two core components. First, we design a pipeline that transforms user interactions—comprising natural-language instructions and subsequent feedback—into high-quality, in-distribution training data. This process bridges the gap between curated datasets and authentic deployment language, enabling agents to continually refine their understanding of both instruction following and navigation behavior. Second, we introduce a memory-bank-based warm-start mechanism that retains accumulated environmental knowledge to provide stronger initialization during redeployment, mitigating the performance degradation typically observed when models are re-initialized in fixed environments. By combining user-driven data construction with memory-driven warm start, our framework enables agents to continuously improve throughout long-term deployment

rather than remaining constrained by static training data.

Our main contributions are summarized as follows:

- **Extension beyond GSA-VLN.** Building upon GR-DUET, we extend the adaptation paradigm beyond GSA-VLN by explicitly incorporating user feedback as a new form of supervision, introducing a user-feedback-driven framework for VLN.
- **User-feedback-driven data construction.** We propose the first pipeline that systematically converts user instructions and corrective feedback into high-quality, in-distribution training data, improving adaptability to realistic deployment conditions.
- **Memory-bank warm start.** We develop a memory-bank mechanism that preserves and reuses accumulated environmental knowledge, enabling stronger initialization during redeployment and mitigating cold-start degradation.
- **Comprehensive evaluation under realistic settings.** Extensive experiments inspired by long-term deployment scenarios demonstrate that our method consistently outperforms strong baselines and supports continual learning in practical navigation tasks.

## II. RELATE WORK

### A. General VLN

Vision-and-Language Navigation (VLN) was first introduced by the Room-to-Room (R2R) dataset [1], which established the fundamental task of “navigating in indoor environments based on natural language instructions.” Subsequent work expanded the scale and difficulty of datasets, such as Room-Across-Room (RxR) [2], which provided multilingual instructions, longer trajectories, and fine-grained descriptions; REVERIE [9], which emphasized object-level navigation; and SOON [20], which focused on navigation involving functional object categories. In addition, VLN-CE [11] extended the task from discrete viewpoints to continuous navigation spaces, enabling more realistic embodied interactions and bridging VLN with embodied control research.

Recently, General Scene Adaptation for VLN (GSA-VLN) was proposed [19], highlighting the importance of leveraging consistency and repeatability of scenarios in long-term deployment. Alongside this, the GSA-R2R dataset provides diverse instruction styles and both in-domain and out-of-domain test conditions. Building on this, Hong et al. introduced the GR-DUET model, which employs graph-structured memory and dual-scale Transformers, effectively improving scenario-specific adaptation.

Early VLN models were mostly based on attention-augmented LSTM sequence-to-sequence architectures [1], [21]. Later, Transformer-based architectures significantly improved performance, such as Recurrent VLN BERT [22], HAMT [23] and DUET [24], as well as pretrained approaches like PREVALENT [25], AirBERT [26], and web-scale instruction-trajectory augmentation [27], [28]. In terms of memory modeling, research gradually expanded from single trajectory histories to more complex long-term modeling. For example, Memory-Adaptive VLN [7] used dynamic memory

to mitigate noise from historical trajectories, while GR-DUET [19] explicitly maintained graph structures of environments.

### B. Test-Time Adaptation for VLN

Test-Time Adaptation (TTA) has become an important research direction in computer vision [29]. For instance, TENT [30] proposed dynamically adapting models during testing by minimizing prediction entropy, achieving strong results in static tasks like image classification and segmentation. However, directly applying such methods to VLN faces new challenges: navigation involves sequential decision-making, and early mistakes can cascade into later decisions, leading to degraded overall performance [31], [32].

To address this, recent studies have introduced feedback mechanisms into TTA frameworks for VLN. ATENA [33] incorporated feedback signals at the episode level and proposed Mixture Entropy Optimization, which combines pseudo-expert distributions to reduce overconfidence in incorrect actions. Relying solely on entropy minimization can cause the agent to become overconfident in incorrect actions, leading to cumulative errors across the trajectory. To mitigate this issue, ATENA introduced a Self-Active Learning module that allows the agent to request human feedback under uncertainty and rely on self-assessment when confident, thereby reducing annotation effort and improving adaptability. Another work, FeedTTA [34], modeled the adaptation process as a reinforcement learning problem, using binary success/failure feedback signals to update the policy, and employed gradient regularization to balance adaptability (plasticity) and stability.

In addition, the Elastic Adaptation Model (EAM) [35] introduced a source-free online test-time adaptation framework for VLN, which adapts pre-trained agents to new environments using an auxiliary decision model and a sample replay mechanism under an unsupervised setting.

### C. Data Expansion and Self-Evolution for VLN

Another line of research focuses on improving generalization through data expansion. Scaling Data Generation in VLN [8] built large-scale training datasets with synthetic instructions and trajectories, significantly improving performance in cross-environment testing. However, such approaches rely on offline generation, and the language styles and task distributions often fail to cover the diverse instructions produced by real users during deployment [36], [37]. More recently, SE-VLN [38] explored self-evolution with multimodal large models, integrating hierarchical memory, retrieval-augmented reasoning, and self-reflection mechanisms to enable agents to gradually improve through continuous interaction. Nonetheless, most of these approaches rely on internal model loops and have yet to propose systematic pipelines for converting natural user interactions into structured training samples [39].

Despite these advances, existing research leaves an important gap between benchmark-oriented adaptation methods and practical deployment scenarios. Current feedback-driven approaches in VLN mainly operate at the level of coarse, episodic success/failure signals, while data expansion methods rely on offline synthetic generation that does not

reflect the diversity of natural user instructions. Moreover, existing memory-based models preserve environment-specific structures but still lack mechanisms to convert accumulated experience into persistent, reusable knowledge. To the best of our knowledge, little work has explored how to systematically transform natural user interactions—including instructions, corrections, and feedback—into structured training samples that enable continual adaptation in realistic settings. In this paper, we address this gap by introducing a user-feedback-driven data construction pipeline together with a memory-bank warm-start mechanism, thereby enabling embodied agents to continually improve in long-term deployment beyond the conventional GSA-VLN paradigm.

## III. METHOD

### A. Task Definition: VLN and GSA-VLN

In the standard Vision-Language Navigation (VLN) task, an embodied agent executes a natural language instruction in a novel environment without prior exposure. Formally, an instruction is represented as

$$I = (w_1, w_2, \dots, w_L), \quad (1)$$

and the environment is modeled as a connectivity graph  $G = (V, E)$ . The agent begins from an initial viewpoint  $v_0$ , receives observation  $o_t$  at step  $t$ , and selects an action:

$$a_t = \pi_\theta(I, v_t, o_t), \quad (2)$$

where  $\pi_\theta$  is a navigation policy parameterized by  $\theta$ . This process generates a trajectory  $\tau = (v_1, v_2, \dots, v_T)$  that ideally terminates at the target viewpoint  $v^*$  specified by  $I$ . In this conventional formulation, model parameters are fixed during inference, and each episode is independent.

*a) General Scenario Adaptation (GSA-VLN):* The GSA-VLN paradigm extends the VLN setting to more realistic, long-term deployments in which the agent repeatedly operates within the same environment  $E$ . Instead of discarding prior experience, the agent maintains an environment-specific memory that accumulates structural and behavioral knowledge over time:

$$\mathcal{M}_E = \{(I_i, O_i, A_i, P_i)\}_{i=1}^k, \quad (3)$$

where  $I_i$ ,  $O_i$ ,  $A_i$ , and  $P_i$  denote instructions, observations, actions, and paths collected from previous episodes. During subsequent runs, the agent can exploit this memory to inform navigation:

$$a_t = \pi_\theta(I, v_t, o_t, \mathcal{M}_E), \quad (4)$$

and optionally update its parameters through unsupervised learning:

$$\theta' = \theta - \alpha \nabla_\theta \mathcal{L}(\mathcal{M}_E; \theta), \quad (5)$$

where  $\mathcal{L}$  denotes a self-supervised objective computed on stored experience. While this formulation enables environment-driven adaptation, it does not incorporate user interactions as supervision. In contrast, our framework augments GSA-VLN with explicit user feedback , allowing natural corrections to guide continual policy refinement.

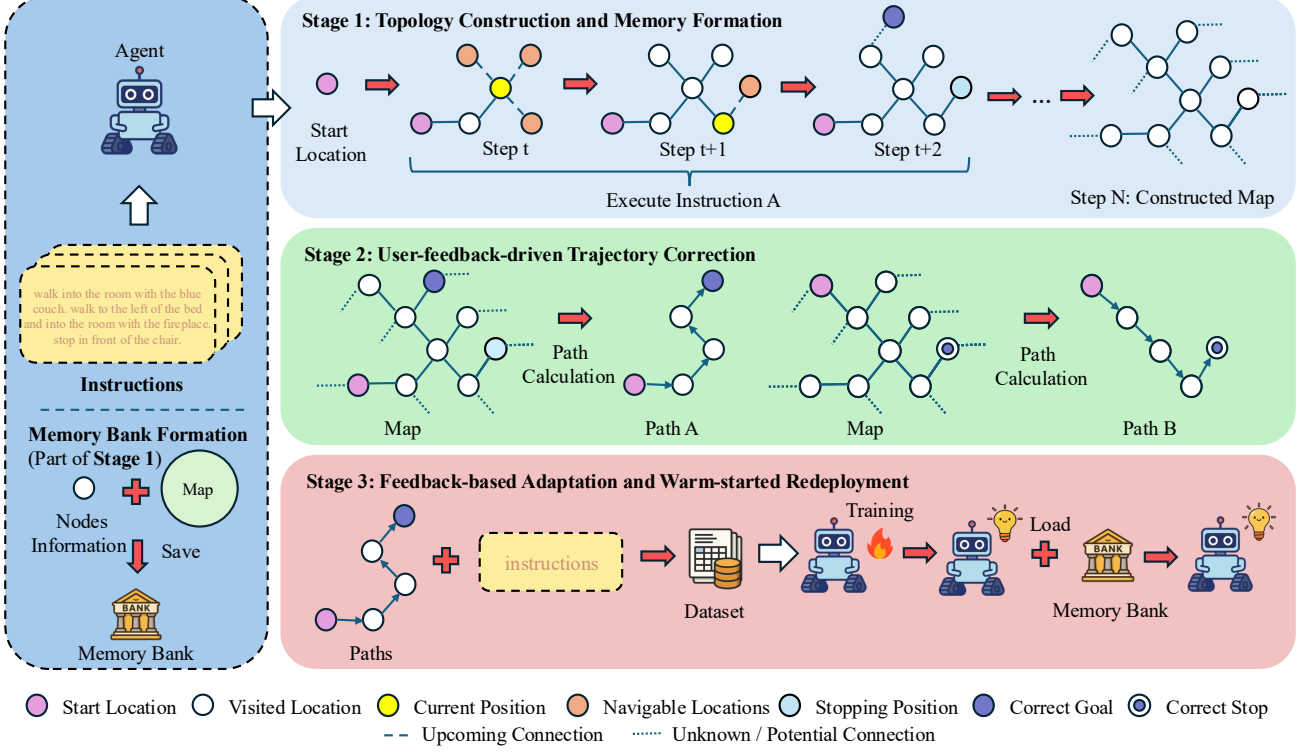


Fig. 2. Overview of the proposed user-feedback-driven adaptation framework for Vision-Language Navigation (VLN). **Stage 1: Topology Construction and Memory Formation.** The agent executes user instructions while incrementally building a topological map of the environment. The dashed lines ..... represent unknown (e.g., Step t+2) or potential (e.g., constructed map) connections. **Stage 2: User-feedback-driven Trajectory Correction** When the agent stops at an incorrect location, the user specifies the correct goal **Correct Goal**. The corrected trajectory is computed via A\* search on the constructed topology. **Stage 3: Feedback-based Adaptation and Warm-started Redeployment.** The corrected instruction-trajectory pairs are aggregated to fine-tune the policy using the DAgger framework. During redeployment, the agent reloads the memory bank, which stores the environment topology and cached note information, to enable warm-start initialization and mitigate cold-start degradation.

### B. Stage 1: Topology Construction and Memory Formation

In GSA-VLN, the environment remains fixed across episodes, allowing the agent to incrementally construct a topological representation that captures spatial connectivity and viewpoint relations. Following GR-DUET [19], we maintain an environment-level memory, but extend it to be *persistently reloadable* across deployments. Specifically, we define

$$\mathcal{M}_E = (G_E, \mathcal{C}_E, \mathcal{S}_E), \quad (6)$$

where  $G_E = (V_E, E_E)$  is the discovered topological graph,  $\mathcal{C}_E$  denotes cached panoramic inputs associated with viewpoints (e.g., image and positional features, navigation types, and view lengths), and  $\mathcal{S}_E$  records candidate-viewpoint mappings that facilitate action conversion during navigation.

At time  $t$ , the policy uses the current instruction and viewpoint together with the cached inputs retrieved from the memory:

$$a_t \sim \pi_\theta(I, v_t, \text{inputs}(v_t; \mathcal{C}_E), G_E), \quad (7)$$

where  $\text{inputs}(v_t; \mathcal{C}_E)$  fetches cached panoramic features for  $v_t$  (or computes them if absent). This enables efficient execution without redundant feature extraction, while maintaining full compatibility with GR-DUET's architecture.

### C. Stage 2: User-feedback-driven Trajectory Correction

After executing an instruction  $I$ , the agent produces a trajectory

$$\tau = (v_1, v_2, \dots, v_T), \quad (8)$$

ending at viewpoint  $v_T$ . The user then provides feedback: if  $v_T$  correctly matches the target, the trajectory is accepted; otherwise, the correct goal viewpoint  $v^*$  is specified.

As illustrated in Stage 2 of Fig. 3, when feedback indicates an error, the corrected path is computed using the A\* algorithm on the existing topological graph:

$$\tau^+ = \text{A}^*(v_1 \rightarrow v^*, G_E). \quad (9)$$

Each corrected pair  $(I, \tau^+)$  is stored as a new adaptation sample. To ensure data quality, we remove cases where  $\tau^+$  is too short ( $< 5$  nodes) or too long ( $> 7$  nodes), as these often indicate incomplete topology or inconsistent feedback.

This design transforms minimal user supervision—simply specifying the final viewpoint—into high-quality, in-distribution training data. Compared with unsupervised GSA-VLN adaptation, the resulting dataset provides explicit semantic alignment with user intent, effectively bridging the gap between synthetic instructions and real-world interaction data.

#### D. Stage 3: Feedback-based Adaptation and Warm-started Redeployment

Once corrected trajectories are accumulated, we form an adaptation dataset:

$$\mathcal{D}_{adapt} = \{(I_i, \tau_i^+)\}_{i=1}^N. \quad (10)$$

The navigation policy is then fine-tuned using the standard imitation learning objective adopted in GR-DUET:

$$\mathcal{L}_{IL} = -\frac{1}{N} \sum_{(I, \tau^+) \in \mathcal{D}_{adapt}} \sum_{t=1}^{|\tau^+|} \log \pi_\theta(a_t^+ | v_t, I), \quad (11)$$

where  $a_t^+$  is the oracle action from the corrected trajectory  $\tau^+$ . This objective aligns the policy with user feedback without modifying the base model's optimization procedure.

1) *Memory-bank Warm Start*: After fine-tuning, the agent is redeployed in the same environment. Instead of reconstructing the graph and visual features from scratch, it reloads the previously stored memory  $\mathcal{M}_E = (G_E, \mathcal{C}_E, \mathcal{S}_E)$ , enabling immediate reuse of environment topology and cached representations. This *reloadable memory* extends the GR-DUET design by introducing persistent scene states that can be saved and restored across sessions, maintaining structural and perceptual continuity during redeployment.

Although the memory-bank warm start does not alter the training objective, it provides a practical advantage for long-term operation. By retaining environment-specific knowledge acquired in previous runs, it stabilizes early-stage navigation and mitigates cold-start degradation that often occurs after model updates. This persistent memory thus serves as a lightweight yet effective mechanism to enhance robustness and ensure smooth adaptation across continual and hybrid deployment settings.

2) *Continual Adaptation*: In long-term deployment, an agent interacts with multiple users sequentially over time. To enable continuous improvement, we perform incremental parameter updates as new feedback data  $\mathcal{D}_{adapt}^{(t)}$  are collected at time  $t$ :

$$\theta_{t+1} = \theta_t - \alpha \nabla_\theta \mathcal{L}_{IL}(\theta_t; \mathcal{D}_{adapt}^{(t)}), \quad (12)$$

where  $\alpha$  is the learning rate. This continual adaptation mechanism allows the agent to gradually integrate feedback from successive interactions, aligning its behavior with both evolving user language and environment familiarity.

3) *Hybrid Adaptation*: In practical multi-user deployments, several users may interact with the same agent concurrently in one environment. To handle such concurrent supervision efficiently, we introduce *hybrid adaptation*, which aggregates feedback from all users within a deployment window:

$$\mathcal{D}_{hybrid} = \bigcup_{u=1}^U \mathcal{D}_u, \quad \theta' = \arg \min_{\theta} \mathcal{L}_{IL}(\theta; \mathcal{D}_{hybrid}), \quad (13)$$

where  $\mathcal{D}_u$  represents feedback-corrected trajectories from user  $u$ . By jointly optimizing across multiple user datasets, hybrid adaptation captures diverse linguistic expressions and navigation styles while avoiding bias toward early interactions. Together, continual and hybrid adaptation mechanisms enable

the agent to evolve both temporally and socially in long-term, multi-user environments.

By integrating user-feedback-driven dataset construction, imitation-based policy adaptation, and a reloadable memory bank derived from GR-DUET, our framework transforms deployment experience into a sustainable learning loop. The agent continuously improves its navigation ability while efficiently reusing previously explored structural and visual knowledge—achieving adaptive, stable performance beyond static GSA-VLN paradigms.

## IV. EXPERIMENTS

### A. Experimental Setup

a) *Datasets and environments*: We conduct experiments on the GSA-R2R dataset [19], which extends the standard Room-to-Room (R2R) benchmark [1] to support scenario adaptation. In this work, we focus on the *residential environments* and evaluate on two instruction styles: Basic and User. This setting captures the most common real-world deployment scenarios, where navigation agents repeatedly operate in household layouts and encounter both neutral and user-specific language patterns.

b) *Baselines*: We adopt GR-DUET [19] as our primary baseline, since it represents the state of the art for GSA-VLN by explicitly maintaining a global navigation graph for adaptation. To further validate the generality of our approach, we also test other representative VLN methods under the GSA-VLN protocol, including DUET [24], HAMT [23], and NaviLLM [40]. These methods were originally developed for the standard zero-shot VLN setting, and their performance in the adaptation scenario serves as an additional reference.

c) *Implementation details*: Our method builds on GR-DUET as the backbone. We preserve its model architecture and loss formulation, and introduce our feedback-driven dataset construction and memory-bank warm start modules. We adopt the DAgger algorithm during training. At each iteration, the agent executes instructions using a mixture of its current policy and exploration sampling, while an expert oracle provides optimal actions for each encountered state. The expert policy can be configured to use either shortest path distances (SPL) or normalized Dynamic Time Warping scores (nDTW) to evaluate action quality relative to the ground truth trajectory. The policy is then updated using imitation learning on the aggregated state-action pairs from both expert demonstrations and student rollouts.

d) *Adaptation settings*: All adaptation experiments share consistent optimization and hardware settings. Each adaptation stage consists of 30,000 episodes with a batch size of 2, corresponding to approximately 60,000 optimization steps. Training is conducted on a single NVIDIA RTX 4090 GPU for about 5 days per stage.

During adaptation, the agent is trained on a mixture of user-feedback data and source-domain data (i.e., R2R and augment dataset used by GR-DUET). This mixed-domain replay helps stabilize adaptation and mitigates overfitting to user-specific language, thereby maintaining general navigation capability while learning from user-feedback data.

TABLE I

PERFORMANCE COMPARISON ON THE GSA-BASIC TEST SET. HIGHER SR, ORACLE SR, SPL, NDTW, SDTW, AND CLS INDICATE BETTER RESULTS; LOWER NE, ORACLE ERROR, AND PATH LENGTH INDICATE BETTER EFFICIENCY AND PRECISION. BEST RESULTS ARE HIGHLIGHTED IN **BOLD**.

Method	SR↑	Oracle SR↑	SPL↑	NE↓	Oracle Error↓	PL↓	nDTW↑	SDTW↑	CLS↑
HAMT [23]	40.12	46.25	38.23	5.74	3.97	7.72	55.54	34.06	56.09
NaviLLM [40]	49.92	60.25	43.23	4.65	3.01	10.25	57.15	39.29	56.44
DUET [24]	54.04	65.46	42.26	4.44	2.69	13.53	53.06	38.71	52.13
GR-DUET (baseline) [19]	66.96	76.58	61.22	3.25	2.02	9.80	69.24	56.38	67.18
Ours (w/o Mem)	76.33	83.21	70.99	2.53	1.67	9.03	77.13	66.65	73.55
Ours (w/ Mem)	<b>79.04</b>	<b>85.67</b>	<b>74.40</b>	<b>2.26</b>	<b>1.52</b>	<b>8.81</b>	<b>79.67</b>	<b>69.80</b>	<b>76.42</b>

We consider two adaptation modes under identical optimization settings but with different data scales:

- Continual adaptation. The model undergoes three sequential user-guided updates (e.g., Basic → User A → User B), where each stage uses approximately 500 feedback samples. Across all three stages, the cumulative exposure amounts to about 1,500 feedback samples, resulting in a proportionally longer total training time.
- Hybrid adaptation. The model aggregates feedback from five users into a single adaptation stage with 500 total samples. This one-time adaptation corresponds to the same data scale as a single continual stage, requiring only about one-third of the total training time while providing a compact and efficient adaptation setup.

Unless otherwise specified, all subsequent adaptation experiments follow the above configuration.

### B. Evaluation Metrics

We evaluate navigation performance using standard metrics from the Vision-and-Language Navigation (VNL) literature, covering goal achievement, path efficiency, trajectory fidelity, and semantic alignment. Following the Room-to-Room (R2R) benchmark [1], we report nine widely used metrics: Success Rate (SR) [1], Oracle Success Rate (Oracle SR) [1], Success weighted by Path Length (SPL) [41], Navigation Error (NE) [1], Oracle Error / Oracle Navigation Error [36], Path Length [1], Normalized Dynamic Time Warping (nDTW) [42], Success weighted by nDTW (SDTW) [42], and Coverage weighted by Length Score (CLS) [36]. These metrics are adopted consistently across recent VLN benchmarks [1], [2], [19], [36] to ensure comparability with prior work.

### C. Main Results on the GSA-Basic Test Set

Table I presents the quantitative comparison of different VLN methods on the GSA-Basic test split. We include representative baselines HAMT [23], NaviLLM [40], DUET [24], and GR-DUET [19], where GR-DUET serves as the baseline for our framework. We further evaluate our method under two configurations: (Ours w/o Mem) — the feedback-driven model after adaptation training without memory loading; and (Ours w/ Mem) — the model evaluated with the reloadable memory bank.

From Table I, we observe that traditional transformer-based models such as DUET, NaviLLM, and HAMT exhibit limited performance on the GSA-Basic test split. These methods, originally optimized for static or single-pass VLN settings,

struggle to adapt effectively to the long-term, environment-specific nature of GSA-VLN. In contrast, GR-DUET, which integrates graph-based memory for scene adaptation, provides a much stronger baseline and demonstrates clear advantages over conventional architectures.

Building upon GR-DUET, our proposed user-feedback-driven framework further enhances navigation performance across all evaluation metrics. The feedback-driven variant (Ours w/o Mem) achieves substantial improvement over GR-DUET, showing that incorporating user feedback significantly enhances both navigation success and path efficiency through explicit human-guided policy refinement. Enabling the reloadable memory bank (Ours w/ Mem) yields significant performance gains, demonstrating that previously explored environmental knowledge can be effectively leveraged to overcome the cold-start condition. Without loaded memory, the model begins with limited environmental context, leading to temporarily suboptimal performance that improves as memory is reconstructed during navigation. Overall, these findings suggest that user feedback acts as the primary driver of continual policy improvement, whereas the memory-bank warm-start mechanism offers complementary benefits by mitigating cold-start degradation across deployment cycles. A qualitative visualization in Fig.3 further supports these results: compared to the baseline GR-DUET (left), our user-feedback-adapted model (right) more accurately executes the instruction “walk past the couch and turn left, walk past the stairs and turn right, walk into the room and stop,” successfully reaching the target room. This visual evidence aligns with the consistent improvements across all quantitative metrics in Table I.

### D. Ablation Study

We further analyze how the amount of executed instructions during Stage 1 and the number of user feedback samples during Stage 2 jointly affect the adaptation performance. Table II reports results under different combinations of instruction and feedback quantities on the GSA-Basic test split, using GR-DUET as the reference.

The results show a clear and consistent trend: both instruction execution and user feedback contribute positively to adaptation. Executing more instructions during environment exploration yields denser and more accurate topological graphs, thereby improving spatial understanding. Meanwhile, increasing the number of user feedback samples provides richer and higher-quality supervision, allowing the policy to better align with human intent. Notably, even with only 100

Instruction: walk past the couch and turn left. walk past the stairs and turn right. walk into the room and stop



Fig. 3. Comparison of GR-DUET navigation before (left) and after (right) user-feedback-driven adaptation, showing improved alignment between language instructions and executed trajectory.

feedback samples, our model already surpasses the GR-DUET baseline by a large margin, demonstrating the high sample efficiency of feedback-driven learning. The best performance is achieved when both executed instructions and feedback samples are abundant (500/500), confirming that broader exploration and richer user corrections are complementary and jointly enhance agent adaptation.

These results validate the complementary effects of exploration and feedback in our framework. Increasing the number of executed instructions enhances the agent's spatial under-

standing, while additional feedback further refines its semantic grounding. Even under limited interaction (e.g., 100 feedback samples), the model achieves strong gains, demonstrating that our user-feedback-driven adaptation is both effective and sample-efficient.

#### E. Effect of Executed Instruction Quantity

To further analyze how environment exploration influences adaptation quality, we examine the relationship between the

TABLE II

ABLATION RESULTS ON THE GSA-BASIC SET UNDER DIFFERENT INSTRUCTION AND FEEDBACK QUANTITIES. THE FIRST ROW SHOWS THE **BASELINE (DEFAULT)** CONFIGURATION.

#Instr.	#Fb	SR↑	SPL↑	NE↓	PL↓	nDTW↑	sDTW↑	CLS↑
<b>500</b>	<b>500</b>	<b>76.33</b>	<b>70.99</b>	<b>2.53</b>	9.03	<b>77.13</b>	<b>66.65</b>	<b>73.55</b>
500	300	74.58	69.27	2.62	9.12	75.86	64.75	72.58
500	100	73.83	67.59	2.68	9.26	75.05	63.57	71.48
300	300	74.00	69.45	2.69	<b>8.82</b>	76.16	64.65	72.82
300	100	73.38	68.19	2.80	8.93	74.92	63.77	71.60
100	100	72.29	66.20	2.94	9.59	72.74	61.93	69.77

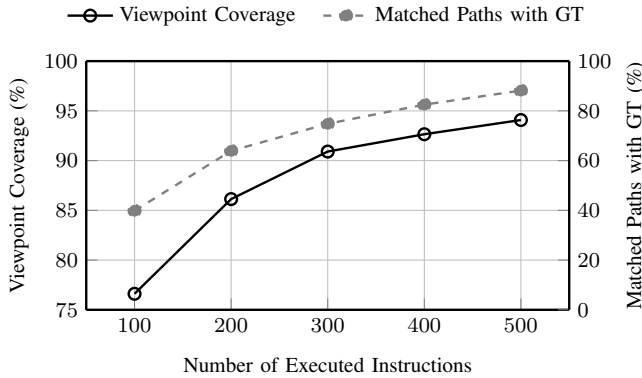


Fig. 4. Effect of executed instruction quantity on both viewpoint coverage (left axis) and matched paths with ground-truth (right axis).

number of executed instructions and two key indicators: viewpoint coverage and matched paths with ground-truth trajectories, as shown in Fig. 4. Viewpoint coverage measures the proportion of unique navigable viewpoints visited during navigation, reflecting the spatial completeness of the constructed topological graph. Matched paths represent the percentage of reconstructed trajectories that correctly align with ground-truth routes. Each executed instruction is accompanied by one corresponding user feedback sample. As the number of executed instructions increases from 100 to 500, both metrics exhibit consistent improvement. Viewpoint coverage rises from 76.61% to 94.08%, indicating that broader exploration leads to more comprehensive spatial representations. Similarly, the proportion of matched paths increases from 39.83% to 88.15%, confirming that richer environmental exposure leads to more accurate reconstruction of ground-truth routes. These trends quantitatively support our claim that more extensive instruction execution enhances environment-specific representation and understanding, providing a stronger foundation for subsequent user-feedback-driven adaptation.

#### F. Continual and Hybrid Adaptation Results

a) *Motivation and setup:* We investigate two complementary user-feedback integration modes that mirror realistic deployment scenarios: (i) **Continual adaptation**, where the model is sequentially updated across multiple users over time (only one active user at a time); and (ii) **Hybrid adaptation**, where feedback from multiple users is aggregated into a single joint update.

TABLE III

CONTINUAL ADAPTATION OVER FIVE RUNS. EACH RUN APPLIES THREE SEQUENTIAL UPDATES: ADAPT-1 (BASIC) → ADAPT-2/3 (RANDOMLY SAMPLED FROM {CHILD, SHELDON, MOIRA, RACHEL, KEITH}). WE REPORT ADAPT-3 RESULTS AND THE GAIN OVER THE *best single-step* AMONG ADAPT-2/3 ( $\Delta^*$ ).

Run	Seq. (Adapt-2/3)	SR	$\Delta^*$	SPL	$\Delta^*$
1	Basic→Rachel→Child	73.00	-0.71	68.79	+0.16
2	Basic→Keith→Rachel	74.29	+0.58	69.19	+0.56
3	Basic→Moira→Keith	72.48	+1.05	67.64	+0.95
4	Basic→Sheldon→Moira	72.52	+0.28	68.85	+1.08
5	Basic→Child→Sheldon	73.95	+1.71	69.13	+1.36
Avg		<b>73.25</b>	<b>+0.58</b>	<b>68.72</b>	<b>+0.82</b>

Notes.  $\Delta^*$ : gain over the *best* one-step fine-tuning among Adapt-2/3.

TABLE IV

AGGREGATE IMPROVEMENT OF CONTINUAL ADAPTATION (ADAPT-3) OVER THE MEAN SINGLE-STEP FINE-TUNING ACROSS {CHILD, SHELDON, MOIRA, RACHEL, KEITH}.

	SR↑	SPL↑	NE (m)↓	nDTW↑	sDTW↑	CLS↑
1-step mean	71.94	67.21	2.69	74.28	62.05	70.98
Adapt-3 mean	73.25	68.72	2.59	75.66	63.77	71.98
$\Delta$	<b>+1.31</b>	<b>+1.51</b>	<b>-0.10</b>	<b>+1.38</b>	<b>+1.72</b>	<b>+1.00</b>

TABLE V

HYBRID ADAPTATION WITH FIVE CONCURRENT USERS. FULL-METRIC COMPARISON AGAINST GR-DUET BASELINE AND CONTINUAL ADAPTATION (ADAPT-3).

Model	SR↑	SPL↑	NE↓	nDTW↑	sDTW↑	CLS↑
GR-DUET	66.96	61.22	3.25	69.24	56.38	67.18
Continual (avg)	<b>73.25</b>	<b>68.72</b>	<b>2.59</b>	<b>75.66</b>	<b>63.77</b>	<b>71.98</b>
Hybrid	71.43	67.22	2.72	74.48	61.96	71.18

Our goal is not to compare them directly, but to demonstrate that the proposed framework remains effective under both deployment conditions.

b) *Continual adaptation:* In this setting, each experiment involves three sequential updates. The first adaptation step uses the *Basic* style (Adapt-1), and the second and third steps (Adapt-2/3) randomly sample from the remaining user styles. Between steps, the policy is incrementally updated using newly collected feedback, resulting in approximately 1,500 feedback samples in total. Table III summarizes results across five independent runs. Despite varying user instruction distributions, the model maintains stable performance (SR std.  $\approx$  0.8, SPL std.  $\approx$  0.6), demonstrating strong robustness. Compared with one-step fine-tuning, continual adaptation consistently improves navigation performance (+1.31 SR, +1.51 SPL, and -0.10 m NE; see Table IV), indicating that progressive user feedback provides complementary learning signals beyond single-step adaptation. Among all sequences, *Basic*→*Keith*→*Rachel* achieves the highest SR (74.29) and SPL (69.19), while *Basic*→*Sheldon*→*Moira* yields the best trajectory alignment with nDTW (76.43) and CLS (72.77).

c) *Hybrid adaptation:* In the hybrid setting, feedback from five users (100 samples each, 500 total) is merged into a single adaptation step. Despite using only one-third of the data and training duration of the continual setup, hybrid adaptation

still yields notable improvements over GR-DUET—+4.47 SR, +6.00 SPL, and  $-0.53$  m NE—with consistent gains across nDTW, SDTW, and CLS (Table V). This demonstrates that multi-user feedback aggregation can provide an efficient and scalable solution for real-world deployments where multiple users interact concurrently under limited training budgets.

Taken together, the two adaptation modes reflect distinct but complementary deployment scenarios—continual adaptation aligns with long-term, sequential user interactions, whereas hybrid adaptation represents concurrent multi-user adaptation within a single update cycle. Across both settings, our framework consistently yields substantial improvements over the GR-DUET baseline in all major metrics, demonstrating its robustness to diverse adaptation conditions and its capacity to effectively integrate user feedback.

## V. CONCLUSION

In this work, we proposed a user-feedback-driven adaptation framework for Vision-and-Language Navigation (VLN), extending the General Scene Adaptation (GSA-VLN) paradigm beyond environment-only learning. Building upon GR-DUET, our framework systematically integrates explicit user feedback into the adaptation process and introduces a memory-bank-based warm-start mechanism for continual deployment. Through extensive experiments on the GSA-R2R benchmark, we demonstrated that: (1) user feedback provides highly effective supervision, substantially improving navigation success and path efficiency even with limited samples; (2) the memory-bank warm start mitigates cold-start degradation during redeployment by reusing environment-specific knowledge accumulated from prior sessions; and (3) both continual and hybrid adaptation modes enable consistent improvements over strong baselines, confirming the practicality of our approach under realistic long-term operation. Our results highlight the importance of leveraging real-world user interaction as a scalable and authentic source of supervision for embodied agents.

## REFERENCES

- P. Anderson, Q. Wu, D. Teney, J. Bruce, M. Johnson, N. Sünderhauf, I. Reid, S. Gould, and A. van den Hengel, “Vision-and-language navigation: Interpreting visually-grounded navigation instructions in real environments,” in *CVPR*, June 2018.
- A. Ku, P. Anderson, R. Patel, E. Ie, and J. Baldridge, “Room-across-room: Multilingual vision-and-language navigation with dense spatiotemporal grounding,” in *EMNLP*, 2020.
- Y. Hong, Q. Wu, Y. Qi, C. Rodriguez-Opazo, and S. Gould, “Vln bert: A recurrent vision-and-language bert for navigation,” in *CVPR*, 2021, pp. 1643–1653.
- S. Wu, X. Fu, F. Wu, and Z.-J. Zha, “Vision-and-language navigation via latent semantic alignment learning,” *IEEE Transactions on Multimedia*, vol. 26, pp. 8406–8418, 2024.
- S. Jeong, G.-C. Kang, S. Choi, J. Kim, and B.-T. Zhang, “Continual vision-and-language navigation,” *arXiv preprint arXiv:2403.15049*, 2024.
- Q. Zheng, D. Liu, C. Wang, J. Zhang, D. Wang, and D. Tao, “Esceme: Vision-and-language navigation with episodic scene memory,” *International Journal of Computer Vision*, vol. 133, no. 1, pp. 254–274, 2025.
- K. He, Y. Jing, Y. Huang, Z. Lu, D. An, and L. Wang, “Memory-adaptive vision-and-language navigation,” *Pattern Recognition*, vol. 153, p. 110511, 2024.
- X. Wang *et al.*, “Scaling data generation in vision-and-language navigation,” in *ICCV*, 2023.
- Y. Qi, Q. Wu, P. Anderson, X. Wang, W. Y. Wang, C. Shen, and A. van den Hengel, “Reverie: Remote embodied visual referring expression in real indoor environments,” in *CVPR*, 2020.
- J. Thomason, M. Murray, M. Cakmak, and L. Zettlemoyer, “Vision-and-dialog navigation,” in *Conference on Robot Learning*. PMLR, 2020, pp. 394–406.
- J. Krantz, E. Wijmans, A. Majumdar, D. Batra, and S. Lee, “Beyond the nav-graph: Vision-and-language navigation in continuous environments,” in *ECCV*. Springer, 2020, pp. 104–120.
- H. Wang, W. Wang, W. Liang, C. Xiong, and J. Shen, “Structured scene memory for vision-language navigation,” in *CVPR*, 2021, pp. 8455–8464.
- S. Zhang, Y. Qiao, Q. Wang, L. Guo, Z. Wei, and J. Liu, “Flexvln: Flexible adaptation for diverse vision-and-language navigation tasks,” *IEEE Transactions on Multimedia*, vol. 27, pp. 6307–6318, 2025.
- T. Yu, Y. Wu, Q. Cui, Q. Huang, and J. Yu, “Mossvln: Memory-observation synergistic system for continuous vision-language navigation,” *IEEE Transactions on Multimedia*, vol. 27, pp. 6690–6704, 2025.
- J. Li, H. Tan, and M. Bansal, “Envedit: Environment editing for vision-and-language navigation,” in *CVPR*, 2022, pp. 15407–15417.
- Y. Hong, Z. Wang, Q. Wu, and S. Gould, “Bridging the gap between learning in discrete and continuous environments for vision-and-language navigation,” in *CVPR*, 2022, pp. 15439–15449.
- C. Huang, O. Mees, A. Zeng, and W. Burgard, “Visual language maps for robot navigation,” *arXiv preprint arXiv:2210.05714*, 2022.
- C.-Y. Ma, Z. Wu, G. AlRegib, C. Xiong, and Z. Kira, “The regretful agent: Heuristic-aided navigation through progress estimation,” in *CVPR*, 2019, pp. 6732–6740.
- H. Hong, Y. Qiao, S. Wang, J. Liu, and Q. Wu, “General scene adaptation for vision-and-language navigation,” in *ICLR*, 2025.
- F. Zhu, Y. Zhu, S. Lu, and X. Liang, “Soon: Scenario oriented object navigation with graph-based exploration,” in *CVPR*, 2021.
- M. Eric and C. D. Manning, “A copy-augmented sequence-to-sequence architecture gives good performance on task-oriented dialogue,” *arXiv preprint arXiv:1701.04024*, 2017.
- Y. Hong, Q. Wu, Y. Qi, C. Rodriguez-Opazo, and S. Gould, “A recurrent vision-and-language bert for navigation,” in *CVPR*, 2021, pp. 1643–1653.
- S. Chen, P.-L. Guhur, I. Laptev, and C. Schmid, “History aware multimodal transformer for vision-and-language navigation,” in *NeurIPS*, 2021.
- S. Chen, M. Tapaswi, P.-L. Guhur, I. Laptev, and C. Schmid, “Think global, act local: Dual-scale graph transformer for vision-and-language navigation,” in *CVPR*, 2022.
- W. Hao, C. Li, X. Li, L. Carin, and J. Gao, “Towards learning a generic agent for vision-and-language navigation via pretraining,” in *CVPR*, 2020.
- P.-L. Guhur, M. Tapaswi, S. Chen, I. Laptev, and C. Schmid, “Airbert: In-domain pretraining for vision-and-language navigation,” in *ICCV*, 2021.
- A. Majumdar, A. Shrivastava, S. Lee, P. Anderson, D. Parikh, and D. Batra, “Improving vision-and-language navigation with image-text pairs from the web,” in *ECCV*, 2020.
- A. Kamath, P. Anderson, S. Wang, J. Y. Koh, A. Ku, A. Waters, Y. Yang, J. Baldridge, and Z. Parekh, “A new path: Scaling vision-and-language navigation with synthetic instructions and imitation learning,” in *CVPR*, 2023, pp. 10813–10823.
- J. Gao, X. Yao, and C. Xu, “Fast-slow test-time adaptation for online vision-and-language navigation,” *arXiv preprint arXiv:2311.13209*, 2023.
- D. Wang, E. Shelhamer, S. Bai, Z. Liu, T. Darrell, A. Gholami, and K. Keutzer, “Tent: Fully test-time adaptation by entropy minimization,” in *ICLR*, 2021.
- S. Ross, G. Gordon, and D. Bagnell, “A reduction of imitation learning and structured prediction to no-regret online learning,” in *Proceedings of the fourteenth international conference on artificial intelligence and statistics*. JMLR Workshop and Conference Proceedings, 2011, pp. 627–635.
- S. Bengio, O. Vinyals, N. Jaitly, and N. Shazeer, “Scheduled sampling for sequence prediction with recurrent neural networks,” *Advances in neural information processing systems*, vol. 28, 2015.
- S. Kim, J. Ko *et al.*, “Atena: Active test-time vision-and-language navigation,” in *arXiv preprint arXiv:2506.06630*, 2025.
- S. J. Kim *et al.*, “Test-time adaptation for online vision-language navigation with feedback-based reinforcement learning,” in *ICML*, 2025.
- M. Tan, P. Chen, H. Zhi, J. Mai, B. Rosman, D. Ji, and R. Zeng, “Source-free elastic model adaptation for vision-and-language navigation,” *IEEE Transactions on Multimedia*, vol. 27, pp. 3953–3965, 2025.

- [36] V. Jain, G. Magalhaes, A. Ku, A. Vaswani, E. Ie, and J. Baldridge, “Stay on the path: Instruction fidelity in vision-and-language navigation,” *arXiv preprint arXiv:1905.12255*, 2019.
- [37] Z. Wei, B. Lin, Y. Nie, J. Chen, S. Ma, H. Xu, and X. Liang, “Unseen from seen: Rewriting observation-instruction using foundation models for augmenting vision-language navigation,” *arXiv preprint arXiv:2503.18065*, 2025.
- [38] X. Dong, H. Zhao, J. Gao, H. Li, X. Ma, Y. Zhou, F. Chen, and J. Liu, “Se-vln: A self-evolving vision-language navigation framework based on multimodal large language models,” *arXiv preprint arXiv:2507.13152*, 2025.
- [39] B. Lin, Y. Nie, Z. Wei, J. Chen, S. Ma, J. Han, H. Xu, X. Chang, and X. Liang, “Navcot: Boosting llm-based vision-and-language navigation via learning disentangled reasoning,” *IEEE Transactions on Pattern Analysis and Machine Intelligence*, 2025.
- [40] D. Zheng, S. Huang, L. Zhao, Y. Zhong, and L. Wang, “Towards learning a generalist model for embodied navigation,” in *Proceedings of the IEEE/CVF Conference on Computer Vision and Pattern Recognition (CVPR)*, June 2024, pp. 13 624–13 634.
- [41] P. Anderson, A. Chang, D. S. Chaplot, A. Dosovitskiy, S. Gupta, V. Koltun, J. Kosecka, J. Malik, R. Mottaghi, M. Savva *et al.*, “On evaluation of embodied navigation agents,” *arXiv preprint arXiv:1807.06757*, 2018.
- [42] G. Ilharco, V. Jain, A. Ku, E. Ie, and J. Baldridge, “General evaluation for instruction conditioned navigation using dynamic time warping,” *arXiv preprint arXiv:1907.05446*, 2019.